**Multifunctional PAA and PEG modified $Co_3V_2O_8$ nanoparticles for enhanced RhB degradation, OER activity, and antibacterial activity: Experimental validation and computational insight**

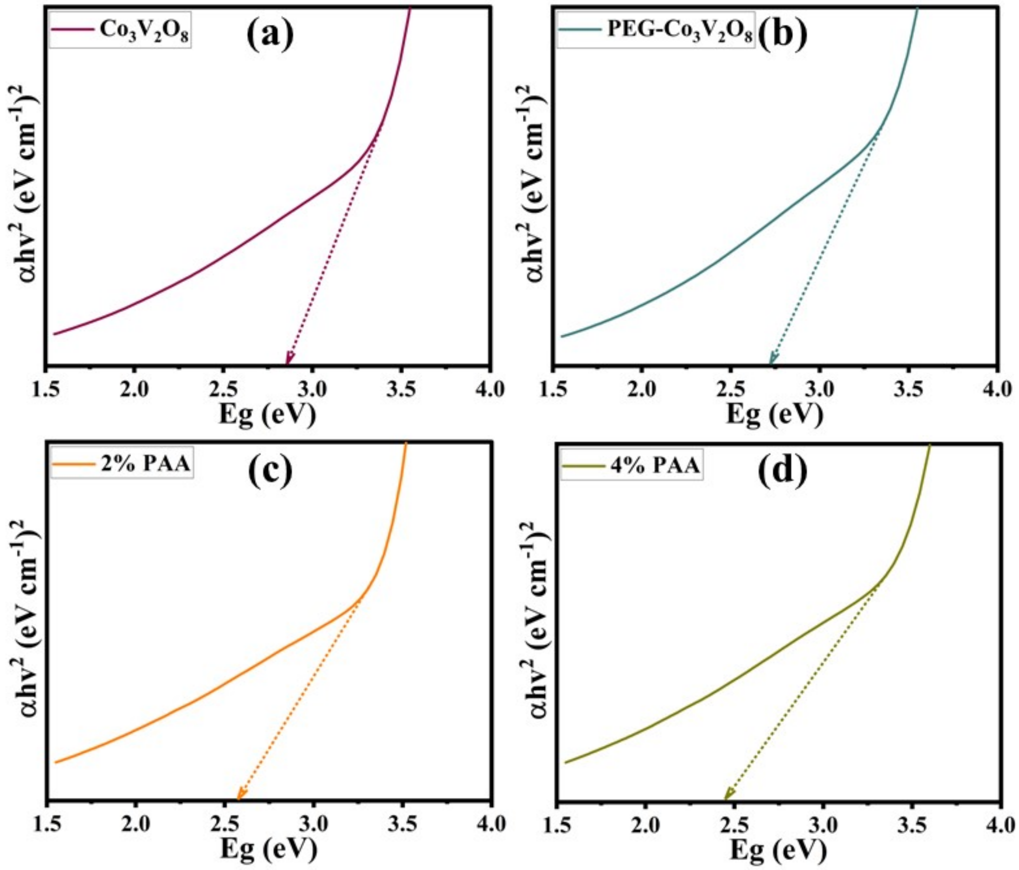


**Figure S1(a-d).** Eg of (a) $Co_3V_2O_8$, (b) PEG-$Co_3V_2O_8$, (c) 2 wt. % of PAA doped PEG-$Co_3V_2O_8$, and (d) 4 wt. % of PAA doped PEG-$Co_3V_2O_8$ NPs

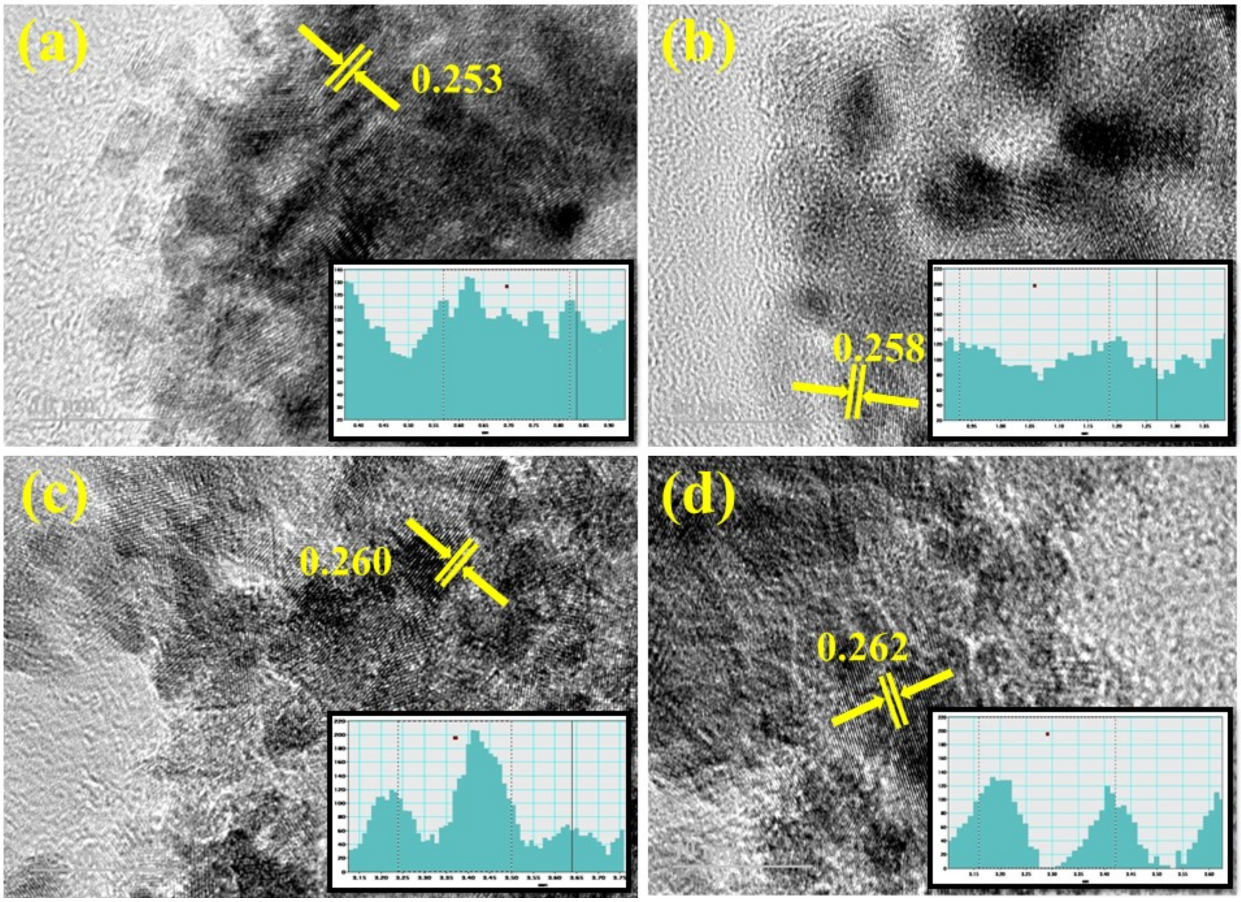


**Figure S2(a-d).** HRTEM images of (a) $Co_3V_2O_8$, (b) 3 wt. % PEG-$Co_3V_2O_8$, (c) 2 wt. % of PAA doped PEG-$Co_3V_2O_8$, and (d) 4 wt. % of PAA doped PEG-$Co_3V_2O_8$ NPs

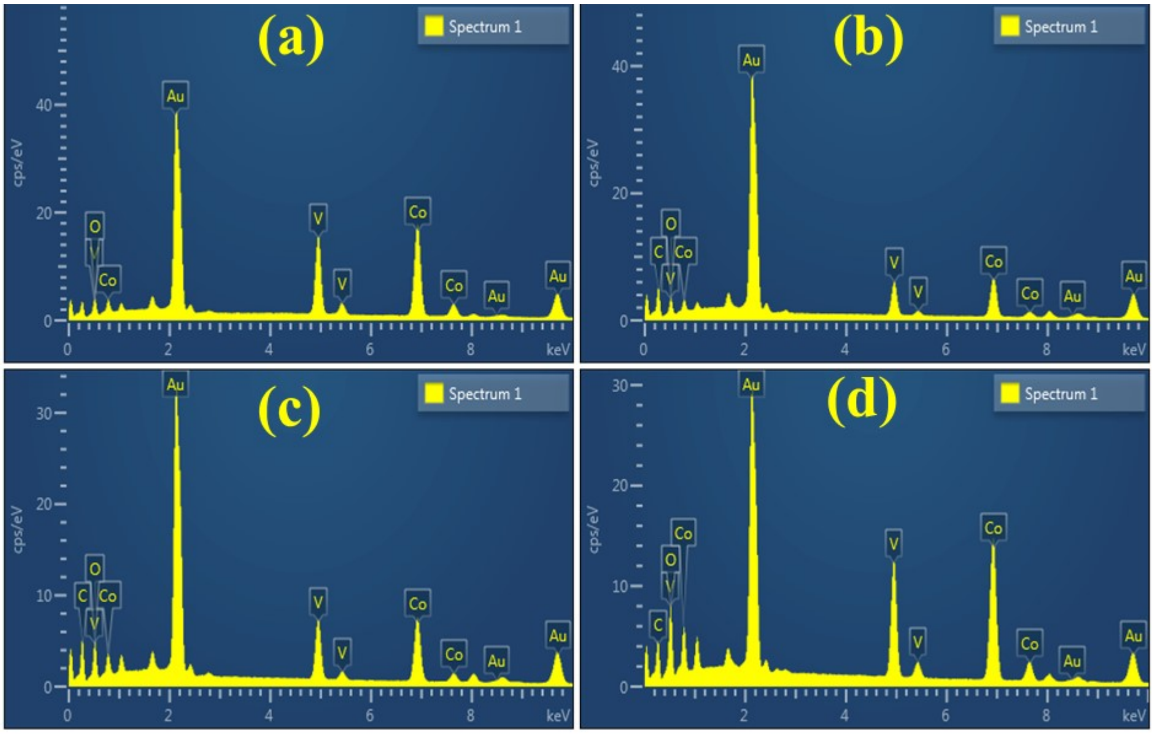


**Figure S3(a-d).** EDS spectra of (a) $Co_3V_2O_8$, (b) 3 wt. % PEG-$Co_3V_2O_8$, (c) 2 wt. % of PAA doped PEG-$Co_3V_2O_8$, and (d) 4 wt. % of PAA doped PEG-$Co_3V_2O_8$ NPs

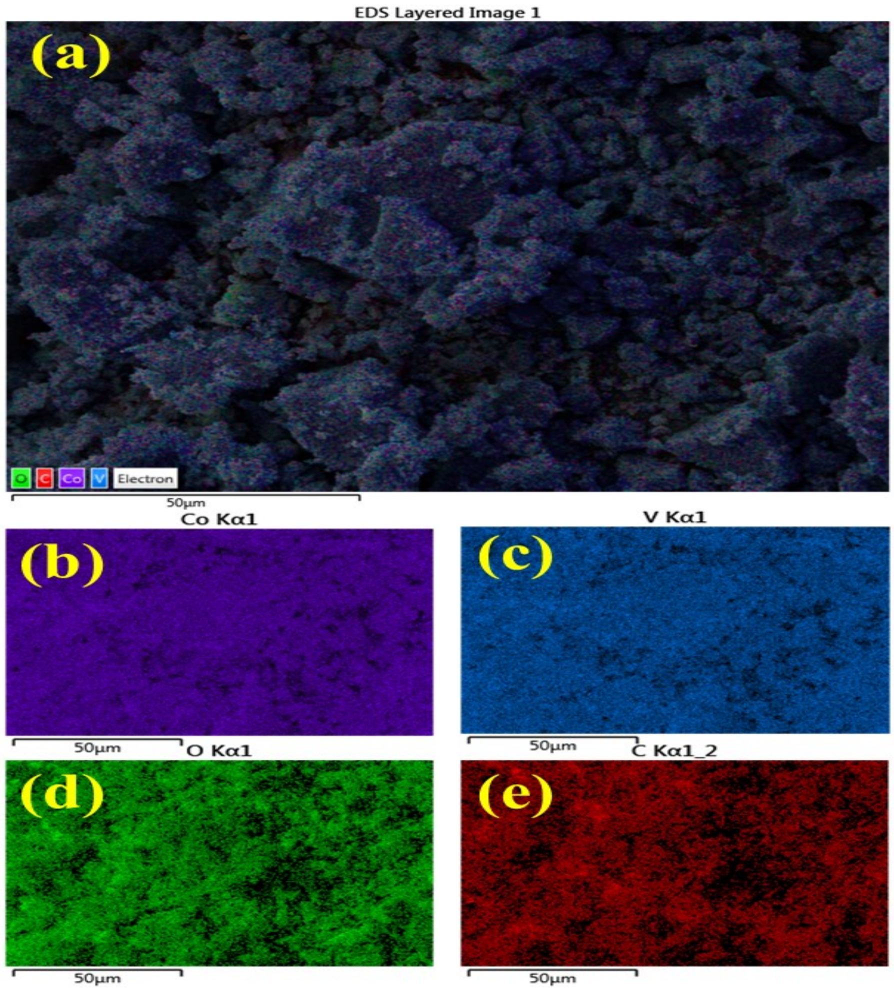


**Figure S4(a-e).** Mapping of 4 wt. % of PAA doped PEG-$Co_3V_2O_8$ NPs

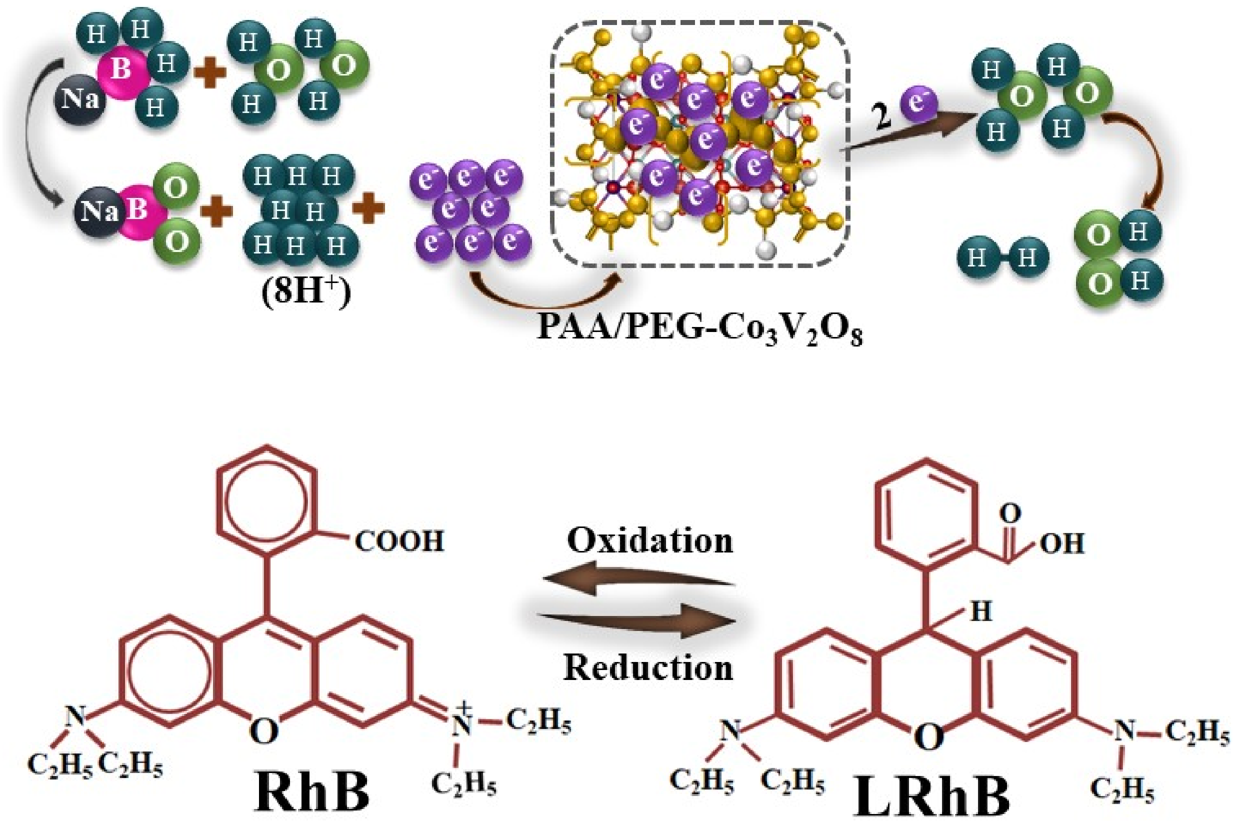


**Figure S5.** Schematic illustration of catalysis mechanism of PAA doped PEG-$Co_3V_2O_8$ NPs

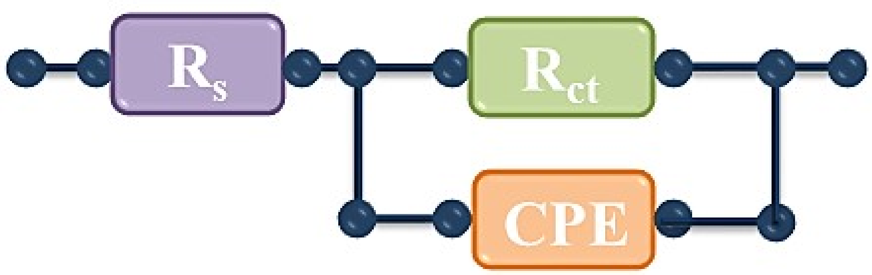


**Figure S6.** EIS fitting model for prepared electrocatalysts

**Table S1.** Resistive parameters of prepared electrocatalyst

| Sample | $R_s$ ($\Omega/cm^2$) | $R_{ct}$ ($\Omega/cm^2$) |
|---|---|---|
| $Co_3V_2O_8$ | 1.03 | 3.06 |

| | | |
|---|---|---|
| PEG-$Co_3V_2O_8$ | 1.19 | 3.50 |
| 2% PAA/PEG-$Co_3V_2O_8$ | 1.09 | 3.12 |
| 4% PAA/PEG-$Co_3V_2O_8$ | 0.97 | 3.02 |

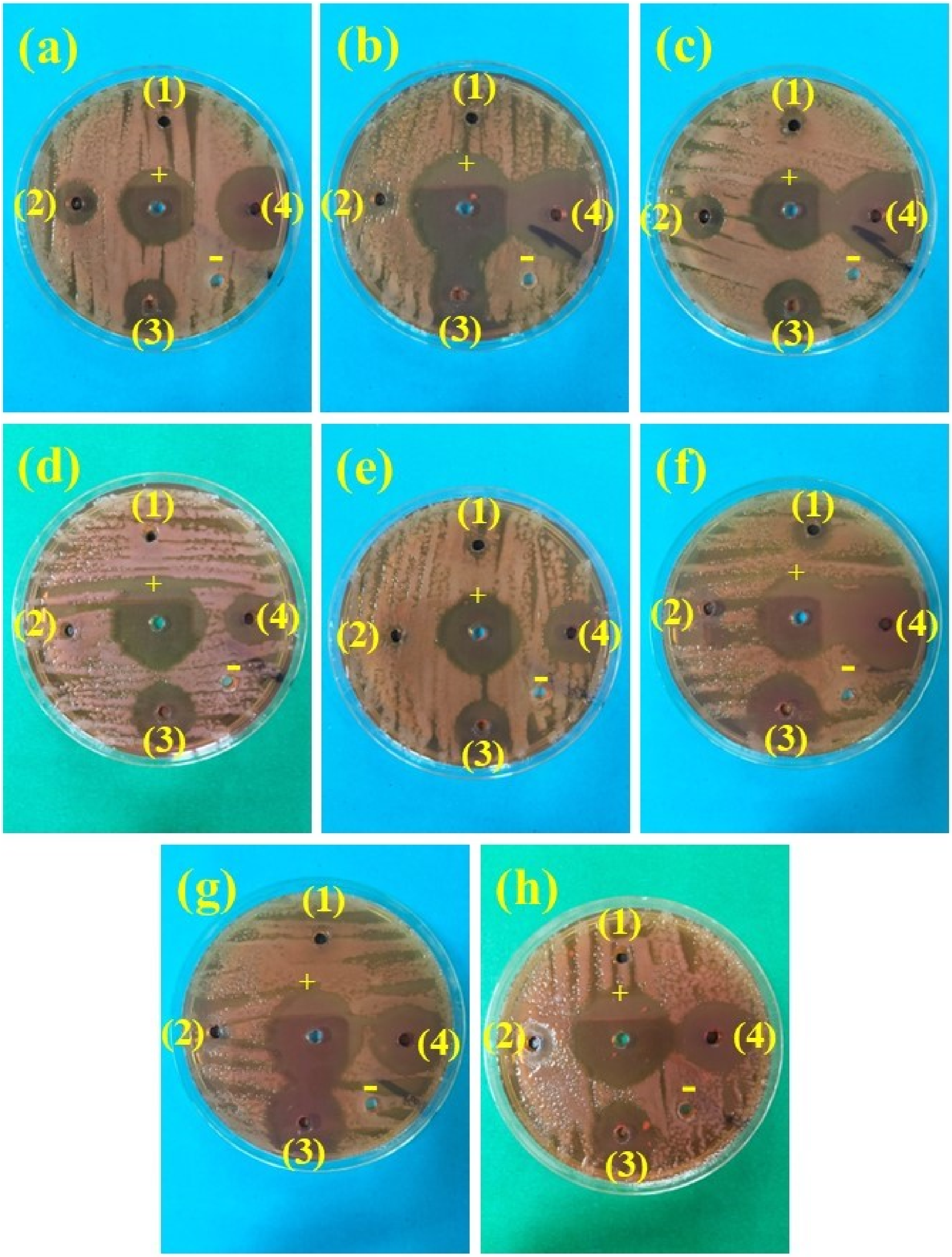


**Figure S7.** In-vitro antibacterial activity of as-synthesized materials on representative isolates at low concentration, whereas 1, 2, 3, and 4 represent $Co_3V_2O_8$, PEG-$Co_3V_2O_8$, 2 wt. % of PAA doped PEG-$Co_3V_2O_8$, and 4 wt. % of PAA doped PEG-$Co_3V_2O_8$, respectively

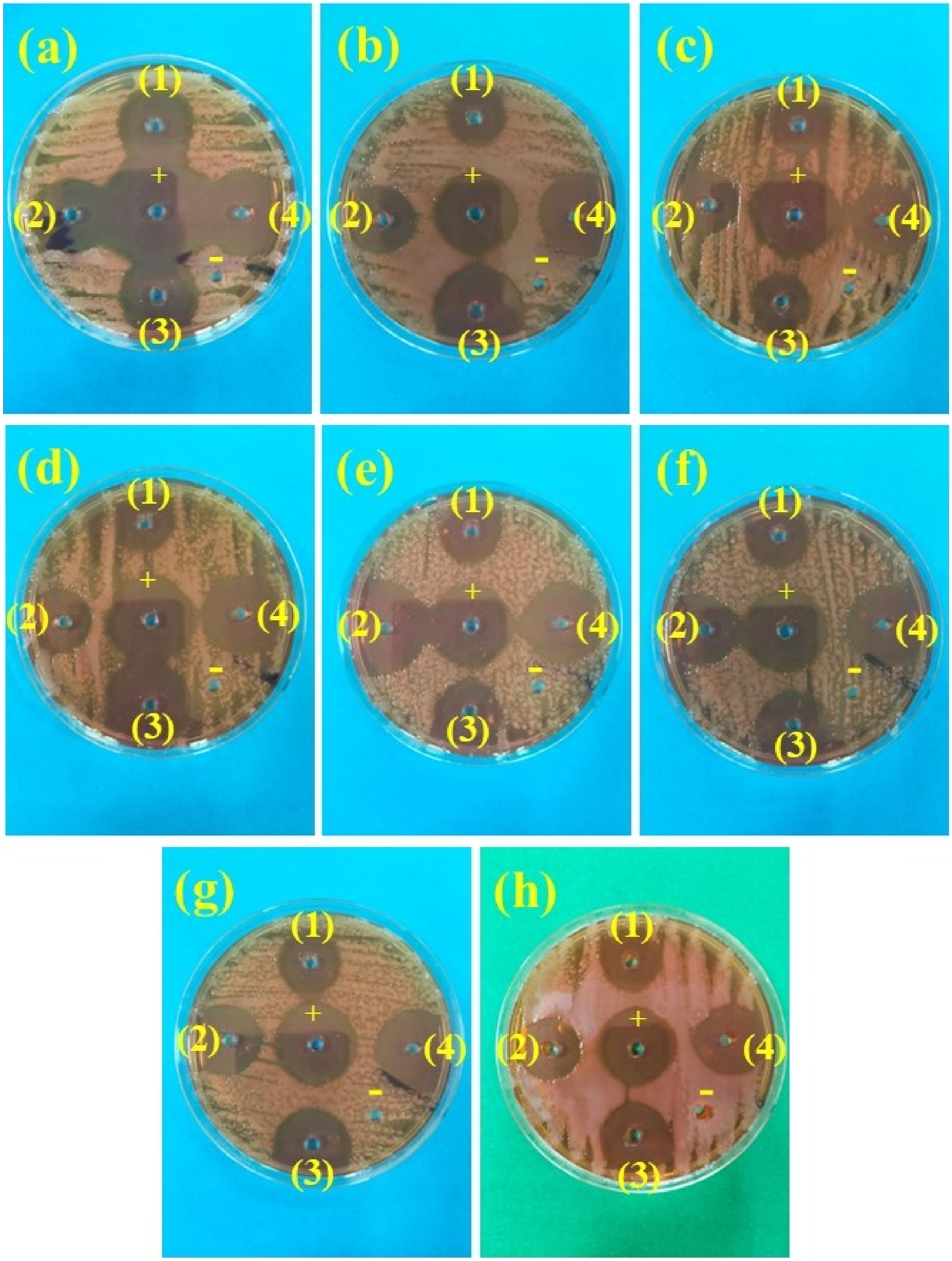


**Figure S8.** In-vitro antibacterial activity of as-synthesized materials on representative isolates at high concentration, whereas 1, 2, 3, and 4 represent $Co_3V_2O_8$, PEG-$Co_3V_2O_8$, 2 wt. % of PAA doped PEG-$Co_3V_2O_8$, and 4 wt. % of PAA doped PEG-$Co_3V_2O_8$, respectively

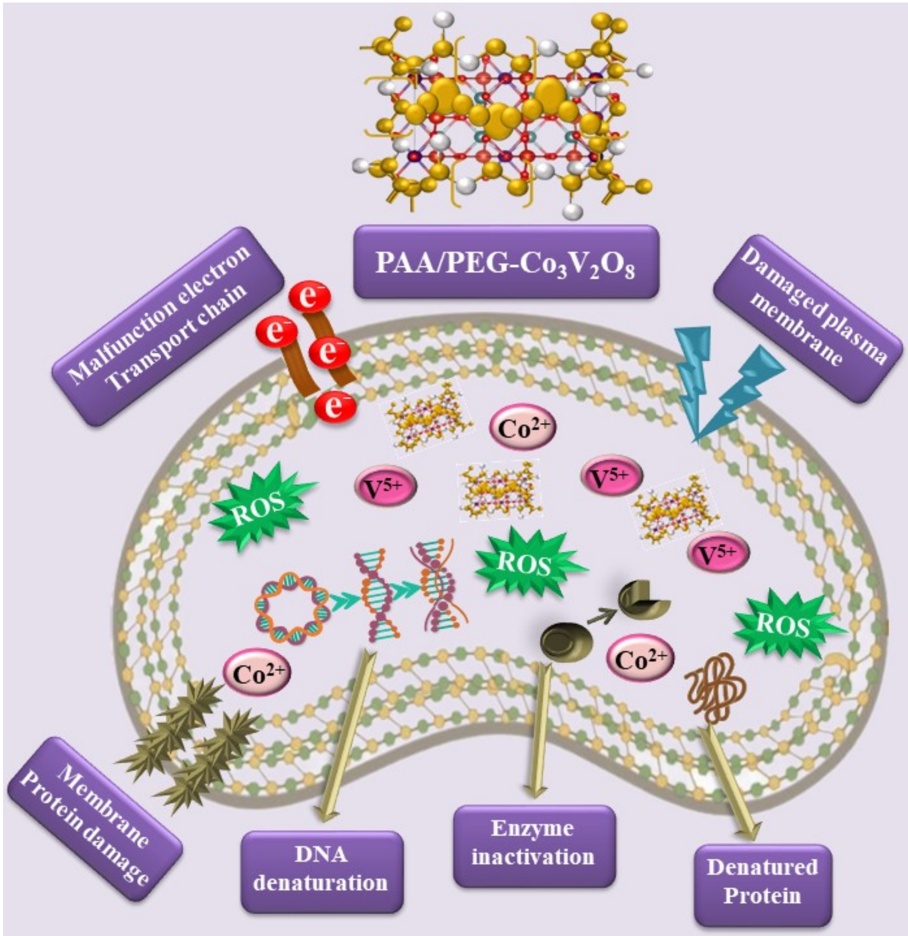


**Figure S9.** Schematic illustration of antimicrobial mechanism of prepared NPs

**Table S2.** Surflex score of docked ligands PAA doped PEG-$Co_3V_2O_8$ NPs bonded to $DHFR_{S.aureus}$ targets.

| Protein | Docking complex | CScore [a] | Crash score[b] | Polar score[c] | G score[d] | PMF score[e] | D score[f] | Chem score[g] |
|---|---|---|---|---|---|---|---|---|
| *DHFR* | $Co_3V_2O_8$ | 5.23 | -0.05 | 5.70 | -30.097 | 3.610 | -111.529 | 8.634 |
| | PEG-$Co_3V_2O_8$ | 6.24 | -0.27 | 5.35 | -104.952 | - 7.068 | -184.157 | 2.224 |

| | | | | | | | | |
|---|---|---|---|---|---|---|---|---|
| *S. aureus* | PAA/PEG-$Co_3V_2O_8$ | 8.62 | -1.97 | 5.09 | -144.225 | 11.292 | -383.945 | 2.656 |
| | Ciprofloxacin | 7.26 | -1.55 | 2.63 | -172.178 | 28.854 | -124.290 | -19.642 |

**Table S3.** Surflex score of docked ligands PAA doped PEG-$Co_3V_2O_8$ NPs bonded to DNA gyrase$_{S.aureus}$ (Topoisomerase II) targets.

| Protein | Docking complex | CScore [a] | Crash score [b] | Polar score [c] | G score [d] | PMF score [e] | D score [f] | Chem score [g] |
|---|---|---|---|---|---|---|---|---|
| *DNA Gyrase* *S. aureus* (Topoisomerase II) | $Co_3V_2O_8$ | 3.57 | -0.12 | 4.93 | -29.719 | - 6.959 | -49.214 | 15.005 |
| | PEG-$Co_3V_2O_8$ | 4.23 | -0.28 | 3.30 | -74.990 | -33.235 | -99.556 | 10.508 |
| | PAA/PEG-$Co_3V_2O_8$ | 4.74 | -1.23 | 4.24 | -103.159 | -39.319 | -199.932 | 8.092 |
| | Ciprofloxacin | 6.73 | -2.44 | 2.30 | -249.863 | -13.351 | -122.376 | -14.031 |

[a]CScore: consensus scoring method employs various scoring functions for affinity of ligands. [b]Crash-score: improper penetration into binding site, [c]Polar region of ligand, [d]G-score for hydrogen bonding, complex (ligand-protein), and internal (ligand-ligand) energies. [e]PMF-score reflects the Helmholtz free energies of interactions for protein-ligand atom pairs (Potential of Mean Force, PMF), while [f]D-score: Charge and van der Waals interactions between ligand-protein. [g]Chem-score for hydrogen bonding, lipophilic contact, and rotational entropy.